Available online at www.sciencedirect.com
SCIENCE DIRECT®
ELSEVIER
Physica B 376–377 (2006) 28–31
PHYSICA B
www.elsevier.com/locate/physb

Pulsed EPR study of spin coherence time of P donors in isotopically controlled Si

Eisuke Abe[a,*], Junichi Isoya[b], Kohei M. Itoh[a,c]

[a]Department of Applied Physics and Physico-Informatics, Keio University, 3-14-1 Hiyoshi, Yokohama 223-8522, Japan
[b]Research Center for Knowledge Communities, University of Tsukuba, 1-2 Kasuga, Tsukuba City 305-8550, Japan
[c]CREST, Japan Science and Technology Agency, 4-1-8 Honcho, Kawaguchi 332-0012, Japan

Abstract

We investigate spin coherence time of electrons bound to phosphorus donors in silicon single crystals. The samples are isotopically controlled so that they may possess various concentrations (from 4.7% to 99.2%) of ^{29}Si, which is the only non-zero-spin stable isotope of silicon. The orientation dependence of electron-spin coherence times are presented, and electron spin echo envelope modulation is analyzed in time-frequency space.

PACS: 03.67.Lx; 28.60.+s; 76.30.−v; 76.60.Lz

Keywords: Electron paramagnetic resonance; Phosphorus-doped silicon; Decoherence; Spin-based quantum computer

1. Introduction

Phosphorus-doped silicon at low temperatures may be one of the most extensively studied material in the field of semiconductor physics. The interest in this material has revived since Kane proposed a silicon-based nuclear spin quantum computer [1], which offers, if realized, an exponential speed-up of a certain type of calculation, such as factorizing a large integer, over present-day LSI processors. The influential Kane proposal has been followed by numerous theoretical considerations of quantum computer schemes based on silicon [2]. As the architectures envisioned in these proposals call for pushing the limit of current silicon technology, experimental progress toward the realization [3] should be fruitful for both classical and quantum computers. On the other hand, when information is processed quantum mechanically (the information unit is often called "qubit"), the problem of decoherence emerges as an inherent roadblock. Decoherence here refers to the process of qubit's losing its transverse coherence, which can occur without energy dissipation to the reservoir. For instance, environmental nuclear spins often cause decoherence of an electron spin by fluctuating the magnetic field in an uncontrollable manner. This is the case for phosphorus electron spins in silicon, because ^{29}Si atoms, one of three stable isotopes of silicon, possess spin $\frac{1}{2}$. It is therefore of particular importance to study how the electron spin coherence is devastated by the ^{29}Si nuclear spins.

The purpose of this contribution is to systematically study the effects of ^{29}Si nuclei, which may be investigated from the following phenomena: (i) electron spin decoherence, as mentioned above, (ii) electron spin echo envelop modulation (ESEEM), and (iii) inhomogeneous broadening of the electron paramagnetic resonance (EPR) lines. The first two are discussed here, while the last one is discussed elsewhere [4].

2. Energy levels

We first review the energy levels associated with an electron bound to a phosphorus nucleus in silicon. Phosphorus has only one stable isotope ^{31}P with nuclear spin $\frac{1}{2}$. At low temperatures, most electrons are captured by the donors and occupy the A_1 orbital ground state, 45 meV

*Corresponding author. Tel.: +81 45 566 1594; fax: +81 45 566 1587.
E-mail address: e-abe@appi.keio.ac.jp (E. Abe).

0921-4526/$ - see front matter © 2005 Elsevier B.V. All rights reserved.
doi:10.1016/j.physb.2005.12.009

beneath the conduction band minimum. Under external magnetic field B_0 along the z axis, the spin Hamiltonian is given by $\mathscr{H} = \omega_e S_z + a\boldsymbol{S}\cdot\boldsymbol{I} - \omega_P I_z$, where $a/2\pi = 118\,\mathrm{MHz}$ is the contact hyperfine constant, and ω_e and ω_P are the Zeeman frequencies of the electron and the nucleus in the given magnetic field, respectively. In the high-field approximation, the energy levels are written as $\omega_e m_S + a m_S m_I - \omega_P m_I$ with $(m_S, m_I) = (\pm\frac{1}{2}, \pm\frac{1}{2})$, and a doublet separated by 4.2 mT appears in the EPR spectrum corresponding to two allowed electron spin transitions ($\Delta m_S = \pm 1$, $\Delta m_I = 0$). Since in the following pulsed X-band EPR experiments microwave pulses excite only one peak of the doublet, we choose without loss of generality the transition with $m_I = -\frac{1}{2}$, and omit m_I from the notation, as depicted in Fig. 1(a). The transition energy is $\tilde{\omega} \equiv \omega_e - a/2 \approx 2\pi \times 9.8\,\mathrm{GHz}$.

Next we add one ^{29}Si nucleus at lth site inside the donor orbital wavefunction. For most of the sites except those adjacent to the origin, it is a fair assumption that the contact hyperfine constant a_l is much smaller than the silicon Zeeman frequency ω_{Si}, and that the dipolar hyperfine coupling is negligible [5]. In this simplified situation, the energy levels are subject to a minor modification $\tilde{\omega} m_S + a_l m_S m_l + \omega_{\mathrm{Si}} m_l$. Hence, the transition energy shifts from $\tilde{\omega}$ by $\pm a_l/2$, as shown in Fig. 1(b). In reality, all the ^{29}Si inside the orbital wavefunction need to be considered. Moreover, the distribution of the nuclei varies randomly from one electron to another, and the measurement is the ensemble average of nearly 10^{14} electron spins. The result is inhomogeneous broadening of the line. The root mean square of the broadening is given as $\sqrt{f\sum_l (a_l/2)^2}$, where the sum runs all the sites except the origin, and $f = 4.7\%$ is the composition ratio of ^{29}Si in natural silicon, or in other words, the probability of finding ^{29}Si at respective sites. The observed linewidth of 0.26 mT has been understood from this expression [5]. Whether this holds for other values of f, larger or smaller than 4.7%, is an interesting and important question, and is addressed in Ref. [4], as suggested in Section 1 (see also the following contribution by Emtsev et al.).

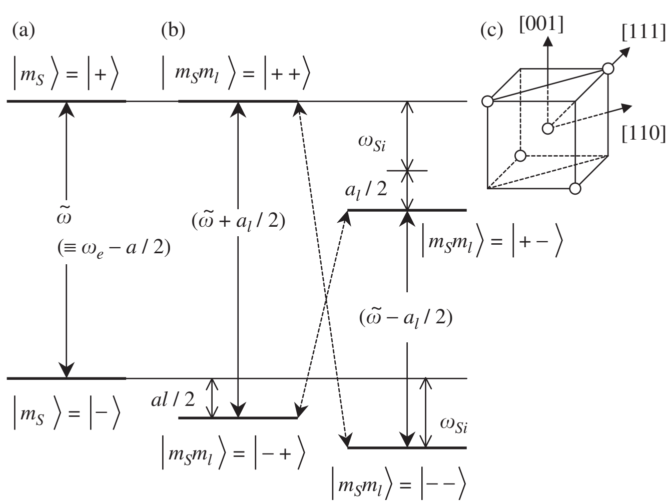

Fig. 1. Energy level diagrams for an electron spin ($S = \frac{1}{2}$) interacting with (a) ^{31}P nucleus ($I = \frac{1}{2}$) and (b) ^{29}Si nucleus ($I = \frac{1}{2}$). (a) Electron spin transition ($\Delta m_S = \pm 1$) when $m_I = -\frac{1}{2}$. (b) Correction due to the addition of one ^{29}Si nucleus at lth site away from the donor ($\omega_{\mathrm{Si}} \gg a_l$). Note that the gyromagnetic ratio of ^{29}Si is negative. The highest energy level is aligned with the upper level of (a) to facilitate the comparison. When the site is adjacent to the donor, the energy differences of $\omega_{\mathrm{Si}} \pm a_l$ may be rewritten as $\omega_\pm$. (c) Schematic showing the tetrahedral configuration of diamond structure.

3. Experimental

In order to systematically investigate the effects of ^{29}Si nuclei, four isotopically controlled silicon single crystals, in which f are, respectively, 4.7%, 10.3%, 47.9% and 99.2%, were prepared. The phosphorus concentrations were of the order of $10^{15}\,\mathrm{cm}^{-3}$, which are low enough to avoid delocalization of the electrons through hopping conduction. Pulsed EPR experiments were carried out using a Bruker Elexsys E580 spectrometer. The sample temperatures were kept at 8K, at which the condition $T_1 \gg T_2$ is fulfilled. A Hahn echo method ($\pi/2$-τ-π-τ-echo) was used, with the $\pi/2$ pulse length of 16 ns. The initial $\pi/2$ pulse creates transverse coherence, or an equal superposition, between up and down spin states. The π pulse applied at τ refocuses spin packets that have different precession frequencies due to the inhomogeneity to form a spin echo at 2τ. The reduction of the echo intensity as increasing τ is the measure of decoherence. The experimental condition and the sample preparation procedure are described in more detail in Refs. [4,6,7].

4. Result and discussion

4.1. Decoherence

In Section 2, we discussed the interaction between the electron and the ^{29}Si nuclei. However, in order to understand the decoherence of the donor electron spins, the dipolar coupling between ^{29}Si nuclei turns out to be essential. Under the condition of energy and momentum conservation, a spin flip of ith nucleus must be accompanied by another spin flip of jth nucleus that is originally in the opposite direction from the former. This "flip–flop" event, driven by $I_i^+ I_j^-$ and $I_i^- I_j^+$ terms in the nuclear dipolar Hamiltonian, changes the total magnetic field felt by the center electron spin by $|a_i - a_j|/2$ (this energy must balance with the dipolar energy) before and after the event. Occurring at random times and positions, the flip–flops cause temporal jumps of the electron Zeeman frequency. The result of accumulation of an unknown relative phase in the superposition state is the loss of transverse coherence: decoherence. The timescale of the nuclear dipolar interaction is of the order of 10^{-4} s; slow compared to the electron spin coherence time itself. Nonetheless, it is responsible for the decoherence because the electron couples to a number of uncontrolled nuclei.

We define the coherence time T_2 as the time at which a Hahn echo envelope decays to $1/e$ of its initial echo intensity. Although this definition applies regardless of the shape of the echo decay curve, owing to the fact that only Gaussian-type decays of the form $\exp(-m\tau^2)$ were observed, we conveniently calculate T_2 as $2/\sqrt{m}$ from the fit to the data. The measurement was repeated as rotating the sample around the $[1\,\bar{1}\,0]$ axis to obtain the orientation dependence of T_2, which is shown in Fig. 2. The maximum T_2 occurs when $B_0 \parallel [0\,0\,1]$, and the minimum when $B_0 \parallel [1\,1\,1]$ for all the samples (see Fig. 1(c) for the lattice configuration). Clearly, this tendency reflects the strength of the nuclear dipolar interaction. That is, when $B_0 \parallel [1\,1\,1]$, one of four tetrahedral bonds of silicon atoms is parallel to B_0, and this pair of nuclei couples so strongly that T_2 becomes shortest. With $B_0 \parallel [0\,0\,1]$, all the dipolar couplings between nearest neighbors are zero thanks to the "magic angle" configuration, hence T_2 is longest. Therefore, we can conclude that the nuclear dipolar couplings significantly contribute to the decoherence of the electron spin in this region of f. A detailed study on f-dependence of T_2 has been carried out by the present authors, and is described elsewhere [4].

Theory on decoherence of localized electron spins surrounded by nuclear spins can be found in Ref. [8], providing good agreement with the present result. Ref. [9] also deals with the same situation, although most of the calculation is devoted to an electron spin confined in a GaAs quantum dot, another candidate system for a solid-state qubit. Currently, coherence time of an electron spin qubit in GaAs double quantum dot structures is measured to be 1.2 μs under small applied magnetic fields [10], and is limited by the hyperfine interaction with the nuclei that fill up the lattice, namely, ^{69}Ga, ^{71}Ga, and ^{75}As all carrying spin $\frac{3}{2}$. Consequently, the dipolar coupling among the nuclei is less important contrary to our case. However, if the coherence time is prolonged at higher magnetic fields or by the use of an efficient electrical pulse sequence, the effect of the nuclear dipolar coupling will become critical.

4.2. Modulation effect

The observation of an echo decay curve is often accompanied by ESEEM. The origin of ESEEM may be explained in terms of state mixing. In Section 2, we implied that the magnitude of a hyperfine interaction could be comparable with ω_{Si} in the vicinity of the donor. In such a case, off-diagonal elements of the Hamiltonian mix up the states $|m_S, m_I\rangle = |\pm\pm\rangle$, and thus m_I is no longer a good quantum number. At this point, we formally rewrite the energy difference between the upper (lower) two states as ω_+ (ω_-), in lieu of $\omega_{\mathrm{Si}} \pm a_I/2$, which are no longer valid. Not to mention, the interpretation that $\omega_\pm$ are the nuclear frequencies shifted by the hyperfine interaction will remain useful. If the bandwidth of the microwave pulse covers $\omega_\pm$, the forbidden transitions ($\Delta m_I = \pm 2$, dashed diagonal arrows in Fig. 1(b)) take place and interfere with the allowed transitions. For instance, if the electrons initially in either of the two lower states are both excited to the same upper state and start to precess, they would interfere each other to imprint a beat of frequency ω_- in an echo decay curve. In the two-pulse ESEEM, the modulation contains frequencies $\omega_\pm$ and $\omega_+ \pm \omega_-$. If more than one nucleus are coupled to the same electron spin, combination frequencies

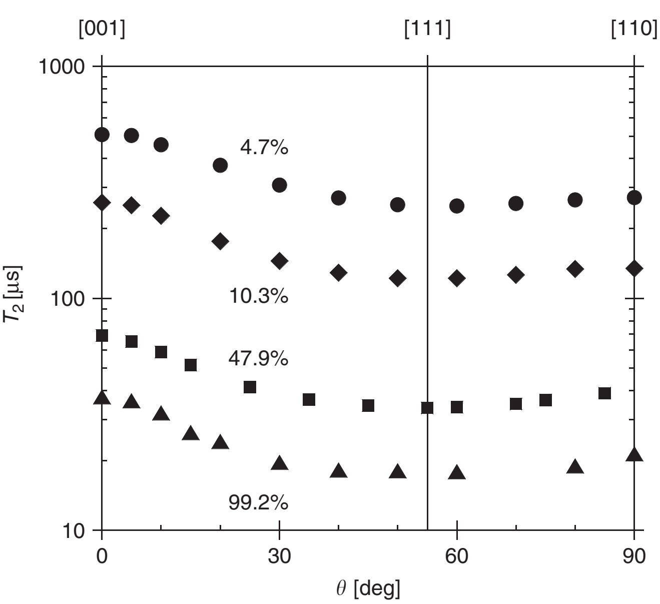

Fig. 2. Orientation dependence of T_2. Circles, diamonds, squares, triangles represent T_2 for $f = 4.7\%$, 10.3%, 47.9%, 99.2%, respectively. θ is defined as the angle between B_0 and $[0\,0\,1]$. See also Fig. 1(c).

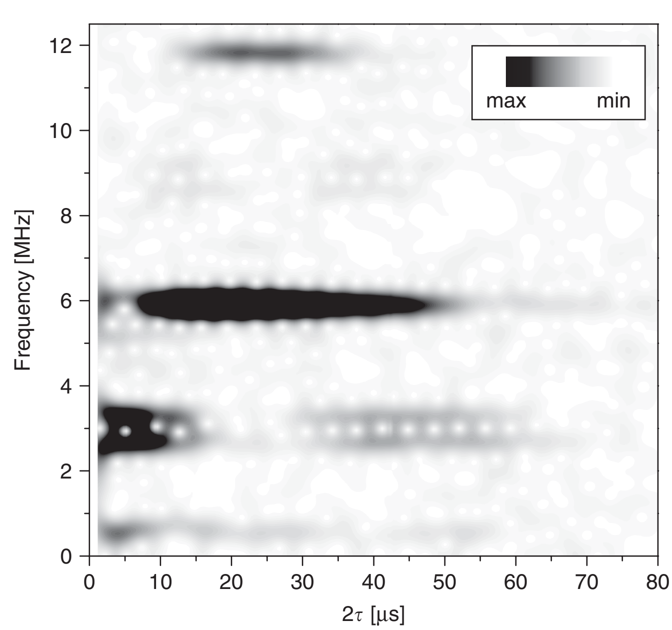

Fig. 3. Time-frequency space analysis of ESEEM in the sample with $f = 99.2\%$ when the external field is applied along $[0\,0\,1]$.

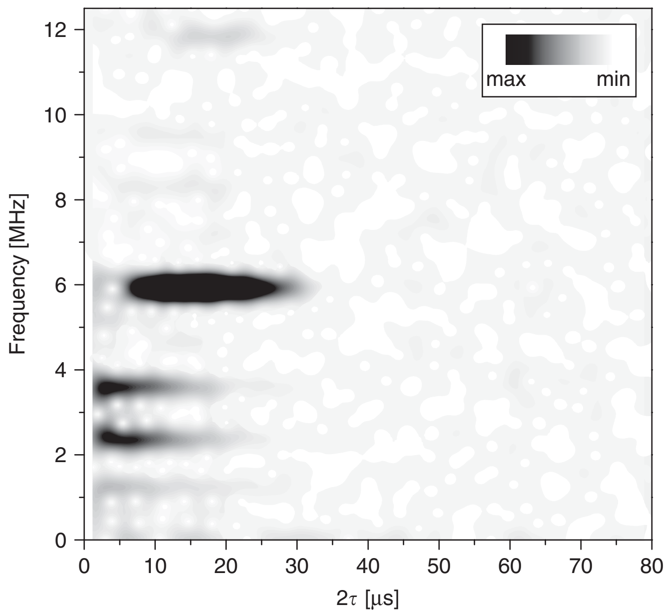

Fig. 4. Time-frequency space analysis of ESEEM in the sample with $f = 99.2\%$ when the external field is applied along [1 1 0].

can also be observed. Analysis of the ESEEM spectra in the frequency domain has been carried out in Ref. [6], in which the modulation was Fourier-transformed after subtraction of the slow decay ($\omega \approx 0$ component). From the analysis of the orientation dependence of the $\omega_\pm$ peaks, it was confirmed that four nearest neighbors of the donor were responsible for the modulation. Here, in order to look at ESEEM from a slightly different perspective, we convert the time domain spectra into continuous wavelet transform chronograms, as shown in Figs. 3 and 4. The former (latter) is for the sample with $f = 99.2\%$ when $B_0 \parallel [0\,0\,1]$ ([1 1 0]). Time-frequency space analysis helps to check how each frequency component evolves in time. It is observed that the orientation-dependent $\omega_\pm$ peaks around 3 MHz, whose shift from $\omega_{\mathrm{Si}}/2\pi$ is due to the hyperfine interaction, appear first and the $\omega_+ + \omega_-$ peak at 6 MHz and the weak higher-order harmonic at 12 MHz subsequently follow. The $\omega_+ + \omega_-$ peak dominates the spectra at later times. Qualitatively, this means that the electron's dipolar field felt by the nuclei with the frequency ω_+ and by those with ω_- are opposite in its direction, and their sum frequency $\omega_+ + \omega_-$ thus cancels this dipolar effect. The faster decay in Fig. 4 than Fig. 3 is due to the faster decay of the echo amplitude itself.

5. Conclusion

In conclusion, we investigated T_2 of the phosphorus-donor electron spins in silicon single crystals, ^{29}Si concentration f of which were varied from 4.7% to 99.2%. The orientation dependence of T_2 indicated that the nuclear dipolar couplings drive the decoherence of the electron spin in this range of f. We also analyzed electron spin echo envelope modulation in time-frequency space.

Acknowledgements

The authors would like to thank A. Fujimoto, S. Yamasaki, and H.-J. Pohl for their contributions. E. A. was supported by Japan Society for the Promotion of Science. This work was partly supported by the Grant-in-Aid for Scientific Research in a Priority Area "Semiconductor Nanospintronics" (no. 14076215).

References

[1] B.E. Kane, Nature 393 (1998) 133.
[2] T.D. Ladd, J.R. Goldman, F. Yamaguchi, Y. Yamamoto, E. Abe, K.M. Itoh, Phys. Rev. Lett. 89 (2002) 017901;
C.D. Hill, L.C.L. Hollenberg, A.C. Fowler, C.J. Wellard, A.D. Greentree, H.-S. Goan, Phys. Rev. B 72 (2005) 045350 and references therein.
[3] J.L. O'Brien, S.R. Schofield, M.Y. Simmons, R.G. Clark, A.S. Dzurak, N.J. Curson, B.E. Kane, N.S. McAlpine, M.E. Hawley, G.W. Brown, Phys. Rev. B 64 (2001) 161401;
T. Sekiguchi, S. Yoshida, K.M. Itoh, Phys. Rev. Lett. 95 (2005) 106101;
T.M. Buehler, V. Chan, A.J. Ferguson, A.S. Dzurak, F.E. Hudson, D.J. Reilly, A.R. Hamilton, R.G. Clark, cond-mat/0506594, unpublished;
T. Shinoda, S. Okamoto, T. Kobayashi, I. Ohdomari, Nature 437 (2005) 1128.
[4] E. Abe, A. Fujimoto, J. Isoya, S. Yamasaki, K.M. Itoh, cond-mat/0512404.
[5] G. Feher, Phys. Rev. 114 (1959) 1219;
E.B. Hale, R.L. Mieher, Phys. Rev. 184 (1969) 739.
[6] E. Abe, K.M. Itoh, J. Isoya, S. Yamasaki, Phys. Rev. B 70 (2004) 033204.
[7] E. Abe, J. Isoya, K.M. Itoh, J. Superconductivity 18 (2005) 157.
[8] R. de Sousa, S. Das Sarma, Phys. Rev. B 68 (2003) 115322;
W.M. Witzel, R. de Sousa, S. Das Sarma, Phys. Rev. B 72 (2005) 161306;
W.M. Witzel, S. Das Sarma, cond-mat/0512323.
[9] W. Yao, R.-B. Liu, L.J. Sham, cond-mat/0508441, unpublished.
[10] J.R. Petta, A.C. Johnson, J.M. Taylor, E.A. Laird, A. Yacoby, M.D. Lukin, C.M. Marcus, M.P. Hanson, A.C. Gossard, Science 309 (2005) 2180. Published online 1 September 2005, doi:10.1126/science.1116955.